Agricultural and Forest Meteorology 180 (2013) 152–163

Contents lists available at SciVerse ScienceDirect

Agricultural and Forest Meteorology

journal homepage: www.elsevier.com/locate/agrformet

Predicting the risk of cedar leaf blight (*Didymascella thujina*) in British Columbia under future climate change

Laura K. Gray[a,*], John H. Russell[b], Alvin D. Yanchuk[c], Barbara J. Hawkins[d]

[a] University of Alberta, Department of Renewable Resources, 751 General Services Building, Edmonton, Alberta T5H 4R1, Canada
[b] British Columbia Forest Service, Cowichan Lake Research Station, Box 335 Mesachie Lake, British Columbia V0R 2N0, Canada
[c] Ministry of Forests, Lands and Natural Resources, Tree Improvement Branch, P.O. Box 9518 STN PROV GOVT, Victoria, British Columbia V8W 9C2, Canada
[d] University of Victoria, Centre for Forest Biology, 151 Cunningham Building, P.O. Box 3020 STN CSC, Victoria, British Columbia V8W 3N5, Canada

ARTICLE INFO

Article history:
Received 26 November 2012
Received in revised form 22 April 2013
Accepted 26 April 2013

Keywords:
Climate envelope modeling
Didymascella thujina
Cedar leaf blight
Climate change
Western redcedar
Forest health

ABSTRACT

Cedar leaf blight (*Didymascella thujina*) is considered to be the most important disease of western redcedar in British Columbia. The disease is most prevalent in warm-moist coastal low-elevation environments causing mortality among seedlings and significant loss of incremental growth and branch death among mature trees. In this study we used a principle component regression model to spatially project the disease risk under observed climate (2003–2008) and multiple future climate scenarios for the 2020s, 2050s, and 2080s. We found that while the majority of future climate scenarios predicted coastal environments will continue to favor occurrence of the disease, intensity is predicted to decrease toward the 2080s. Projected reductions of available summer climate moisture (cumulative precipitation – potential evapotranspiration), corresponding to the time of ascospore discharge and germination, contribute significantly to this finding. Disease intensity is however, projected to increase under moderate temperature and precipitation increases for the 2020s. We therefore recommend current reforestation efforts deploy disease resistant western redcedar seedlots in high risk environments common to hypermaritime coastal regions such as Haida Gwaii and northern maritime, to avoid significant mortality and growth reduction.

1. Introduction

Increased severity of forest disease outbreaks due to climate change has become one of the most significant obstacles to effectively managing commercial forests for the future (Sturrock et al., 2011). It is clear that changes in temperature and precipitation exert strong direct effects on host susceptibility, as well as the survival, reproduction and dispersal of pathogens responsible for disease outbreaks (Ayers and Lombardero, 2000).

For endemic forest pathogens, which are already well established throughout their host distributions, the effect that climate change will have on their range expansion is probably secondary to the changes expected on disease intensity (Dukes et al., 2009). Climate envelope models offer the ability to distinguish the abiotic niche requirements which control endemic pathogens, as well as the ability to project how the frequency and intensity of forest diseases might shift under new climates, based on current observations. Climate envelope models have been used to study climate-forest pathogen interactions for agricultural crops (e.g. Bourgeois et al., 2004), however examples relevant to forest ecosystems are limited. Meentemeyer et al. (2008) used climate envelope models to determine which climate factors and associated species could be used for early detection of sudden oak death caused by the pathogen *Phytophthora ramorum*. Similar studies have expanded this approach to illustrate the vulnerability of *Quercus* dominated ecosystems to *P. ramorum* in the United States (Venette and Cohen, 2006; Kelly et al., 2007; Venette, 2009), and *Phytophthora cinnamomi* in Europe (Bergot et al., 2004) under current and future climate. For a conifer species, Watt et al. (2010) developed a non-linear model to predict infection severity and foliage retention for Swiss needle cast on Douglas-fir under current and future climate in New Zealand.

Predicting how climate change will affect pathogen–host interactions in forest ecosystems is arguably more complex than in agricultural settings due in part to the long-lived nature of trees and the relatively short lifespan of most pathogens. Further, climate envelope models need to be independently generated for infectious agents as pathogen-host interactions are difficult to generalize over multiple organisms. Despite the challenges, it is prudent to continue projecting disease risk in forest ecosystems, especially in locations where both temperature and precipitation

* Corresponding author. Tel.: +1 780 492 2540.
E-mail addresses: lkgray@gmail.com (L.K. Gray), John.Russell@gov.bc.ca (J.H. Russell), Alvin.Yanchuk@gov.bc.ca (A.D. Yanchuk), bhawkins@uvic.ca (B.J. Hawkins).

0168-1923/$ – see front matter © 2013 Elsevier B.V. All rights reserved.
http://dx.doi.org/10.1016/j.agrformet.2013.04.023

are expected to increase. In the absence of water stress, warmer temperatures increase pathogen metabolism, reproductive rates, and survival, leading to disease outbreaks (Boland et al., 2004; Desprez-Loustau et al., 2006; Dukes et al., 2009). In northern British Columbia, severe defoliation and unprecedented mortality of mature native lodgepole pine (*Pinus contorta* var. *latifolia* Dougl. ex Loud.) from epidemic levels of dothistroma needle blight have been related to an increase in summer precipitation for the region which favors the pathogen's development (Woods, 2003; Bradshaw, 2004; Woods et al., 2005). While climate is not anticipated to shift uniformly across British Columbia, mean annual temperature and precipitation are projected to increase on average by as much as 4 °C, and 16%, respectively for the province by the 2050s, with the largest temperature and precipitation increases expected for coastal environments (Murdock and Spittlehouse, 2011). Thus in the future, outbreaks similar to *Dothistroma*, could be observed for other forest diseases in areas throughout the province.

Given western redcedar (*Thuja plicata* Donn ex D. Don) is projected to favor well under future climate change (Gray and Hamann, 2013), it may be important to consider the risk of *Didymascella thujina* (E.J. Durand) Marie (formally *Keithia thujina* E.J. Durand), commonly known as cedar leaf blight on these forest ecosystems. Although the disease is most prevalent in warm-moist environments typical of coastal low elevations of the Pacific Northwest (Russell et al., 2007), the pathogen is endemic to North America and found throughout the natural range of western redcedar (Pawsey, 1960; Sinclair et al., 1987; Kope and Sutherland, 1994).

In natural stands, the cedar leaf blight disease cycle occurs over two growing seasons, with seedlings and young trees being the most susceptible (Pawsey, 1960). In the first growing season, infection of individual leaflets occurs, with disease expression and spread occurring the following year (Trotter et al., 1994). Mature ascospores are discharged from wetted apothecia in the spring and infect leaves of the current growing season. A second ascospore release can potentially occur in the early fall if conditions are wet, and temperatures are above 10 °C (Moore and Green, 1976; Frankel, 1990; Trotter et al., 1994). Mortality of seedlings can be high if the fungus is not treated (Trotter et al., 1994; Kope and Trotter, 1998a; Burdekin and Phillips, 2008) and can significantly impact growth of trees up to 10 years old (Russell et al., 2007). While there is agreement that mortality is rare, infected mature individuals may exhibit significant loss of incremental growth and branch death (Kope et al., 1996). More importantly, cedar leaf blight may be a pioneering fungal pathogen that induces stress on a host tree, allowing infections by secondary pathogens to occur (Russell et al., 2007).

In this study we adopt a climate envelope modeling approach using multivariate regression to investigate the interaction between climate and cedar leaf blight in British Columbia. Although our model is similar to Watt et al. (2010), we use a principal component analysis to remove the collinearity among our selected climate variables while maintaining the environmental space. Further, unlike previous studies (e.g. Meentemeyer et al., 2008; Watt et al., 2010), we do not pre-select or add climate variables to our model based on biological significance, but rather we allow a branch-and bound algorithm to select the set of climate variables which best predicts disease intensity, which we define as the total amount of disease present (Seem, 1984). Often observations of forest disease are collected from performance trials which were not established to investigate forest health issues. Our objective, therefore, is to establish a procedure where this kind of data on any forest disease can be utilized to identify climatic factors that contribute to disease outbreak as well as model disease risk under novel climate conditions. Here, we define risk as the probability of an undesirable outcome (e.g. reduced growth or mortality) due to increased disease levels (Madden et al., 2007).

Cedar leaf blight represents the first forest disease to be modeled and projected under future climate change for British Columbia, and as far as we know, the first using a conifer host and pathogen, both occurring in their native environment. Studies have shown significant variation in cedar leaf blight severity among populations and this variation is related to seed origin such that trees from milder and wetter ecosystems are observed to be more resistant to the disease than other populations planted at the same site (Soegaard, 1956; Porter, 1957; Lines, 1988; Russell et al., 2007; Russell and Krakowski, 2010). The widespread climatic distribution of the host coupled with the clear evidence of strong adaptive variation for resistance to cedar leaf blight among western redcedar natural populations, make this fungal pathogen an informative test case from which to build a modeling procedure.

2. Materials and methods

2.1. Field sites and climate characterization

Six western redcedar populations, each comprised of two to four natural stand seedlots based on similar geographic location, were established as one-year-old seedlings across 36 field sites as part of a larger genetics study (Fig. 1). Each population was represented by 32 seedlings planted in a randomized incomplete block design with one tree per replication. The 36 field sites were established over six years between 1998 and 2004 with four to six sites per year. Severity of leaf blight at ages seven and 10 years was scored on individual trees using a 1–6 scale based on percentage of foliage infected, where 1 = no visual cedar leaf blight and 6 = more than 90% damage. Individual site analyses was undertaken using a linear mixed model, and population mean seven and 10 year scores at each site and for each population were estimated from best linear unbiased estimates (BLUE). The three populations with consistently highest cedar leaf blight scores across all sites were used for all subsequent regression analyses; this was done to avoid underestimating future disease risk. All linear model analyses were performed using ASREML v.3.0 (Gilmour et al., 2009). Geographic and climate characteristics of sites where cedar leaf blight was absent (score = 1) and present (score > 1) are provided in Table 1.

For climatic characterization of the field sites, spatially interpolated climate data was generated using CLIMATE-WNA version 4.62 (http://www.genetics.forestry.ubc.ca/cfcg/ClimateWNA/ClimateWNA.html), which includes a bilinear interpolation of the PRISM (Parameter Regression of Independent Slopes Model) (Daly et al., 2008), along with adjustments in temperature for mountainous terrain (see Hamann and Wang, 2005 for details). Monthly temperature and precipitation surfaces for each field site from 2000 to 2008 were generated using historic climate data observed at Canadian weather stations interpolated as anomalies from the 1961–1990 climate normals (for details see Wang et al., 2012b). Observations have shown that disease incidence is low during the first growing season after infection (Kope and Sutherland, 1994), but becomes conspicuous during the following year as apothecia develop on either the juvenile, needle-like leaves on the stem, or the mature, scale-like leaves on the branches (Kope, 1998). Therefore, climatic factors which initiate or increase measurable blight occurrence are not necessarily reflected in the measurement year. Thus for each field site, climate variables were averaged for the year in which cedar leaf blight measurements were collected, as well as the two previous years. For example, if data collection occurred in 2003 then site climate was averaged for 2001, 2002, and 2003.

Latitude, longitude, elevation, and approximately 75 monthly, seasonal and annual climate variables were considered for model parameterization. Temperature variables included: mean annual temperature, mean warmest month temperature, mean coldest

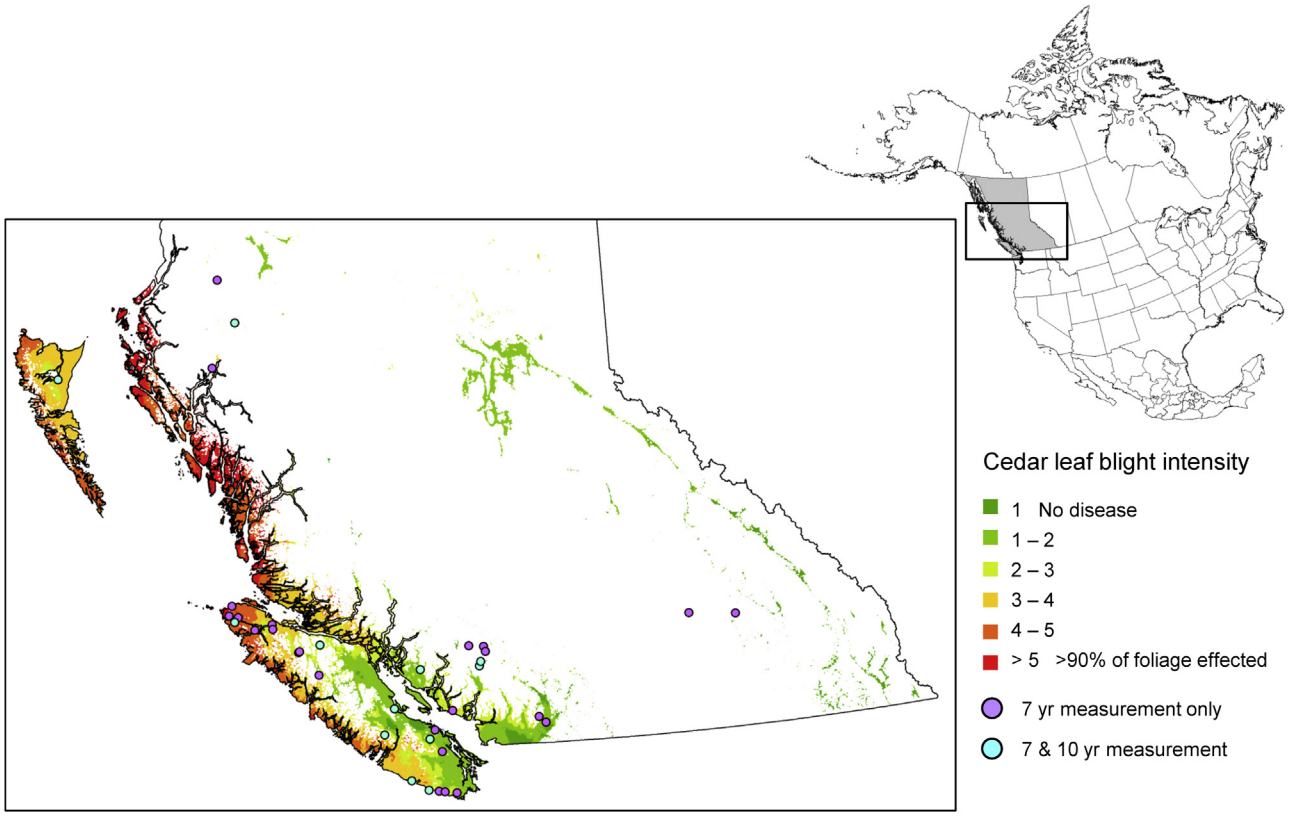

Fig. 1. Cedar leaf blight (CLB) intensity projected under 2003–2008 averaged climate. The locations of western redcedar field progeny test sites are included with year of CLB measurement indicated.

month temperature, continentality (difference between mean January and mean July temperature), number of frost-free days, frost free period, the number of growing degree days above 0 °C and 5 °C, as well as average, minimum and maximum values for each month and season. Similarly, precipitation variables included: mean annual precipitation, mean growing season precipitation (May–September), annual heat moisture index, summer heat moisture index (May–September), and cumulative precipitation for each month and season. All of these variables are described in detail by Wang et al. (2012b). The fungus requires 80–100% relative humidity for at least 12 h for ascospore discharge and germination (Porter, 1957; Kope, 2004). Since humidity measurements were unavailable and cannot be generated for the province under current and future climate scenarios, climate-moisture indices were estimated based on potential evapotranspiration. The four climate-moisture indices (Hogg, 1997) included in variable selection were: annual, spring (April, May, June), summer (June, July, August), and autumn (August, September, October). These indices indicate

Table 1
Mean (±standard deviation), maximum and minimum geographic location, climate and cedar leaf blight intensity for western redcedar field sites with and without cedar leaf blight (CLB), and phenotypic correlations between geographic and climatic variable and cedar leaf blight intensity across all sites. The values in this table reflect climate averaged over the 2003–2008 period when disease observations were collected.

	Variable	CLB absent sites			CLB present sites			Correlation with CLB (r^2)
		Mean	Min	Max	Mean	Min	Max	
Location	Latitude (°)	50.11 ± 1.24	48.94	54.52	50.16 ± 1.81	48.4	55.07	0.19
	Longitude(°)	−123.23 ± 2.29	−128.32	−117.85	−126 ± 2.03	−128.78	−121.98	−0.64
	Elevation (m)	528 ± 291	100	1000	294 ± 243	70	960	−0.44
Climate-general	Mean annual temperature (°C)	6.9 ± 1.9	2.9	9.5	7.9 ± 1.7	2.8	9.4	0.23
	Min winter temperature (°C)[a]	−4.0 ± 3.5	−9.1	0.4	−1.1 ± 2.9	−9.5	1.6	0.42
	Mean annual precipitation (mm)	1699 ± 385	663	2353	2772 ± 764	1303	3995	0.55
Climate- in analysis	Mean summer temperature (°C)	15.2 ± 1.5	11.4	17.1	14.5 ± 1.2	11.4	16.5	−0.31
	Max July temperature (°C)	22.7 ± 1.9	18.3	27.1	20.2 ± 1.9	17.6	23.2	−0.69
	Max August temperature (°C)	21.9 ± 1.6	18.3	25.5	20.1 ± 1.5	17.6	22.4	−0.65
	Summer climate moisture index (cm)	−6.9 ± 4.3	−15.6	0.6	4.8 ± 11.3	−13	27.2	0.75
	Spring precipitation (mm)[b]	335 ± 88	105	498	620 ± 212	187	915	0.5
	Summer precipitation (mm)	181 ± 38	110	235	250 ± 93	110	433	0.63
	May precipitation (mm)	94 ± 29	48	93	200 ± 69	49	191	0.51
	July precipitation (mm)	52 ± 14	29	77	78 ± 32	31	143	0.6
Disease intensity	Cedar leaf blight score (BLUE)[c]	1 ± 0	1	1	2.8 ± 0.8	1.4	4.5	

[a] Winter temperatures were averaged over December, and January and February of the following year.
[b] Spring (March, April, May), summer (June, July, August), May and July precipitation variables are cumulative values.
[c] BLUE: best linear unbiased estimate.

overall humidity of sites and generally correspond to cedar leaf blight ascospore discharge and germination for spring and autumn inoculation events, as well as fungal growth during the summer months (with larger values indicative of humid coastal environments).

2.2. Climate scenarios for British Columbia

Similar to the climate surfaces for the field sites, annual province-wide climate surfaces were generated using observed weather station data interpolated as anomalies from the 1961–1990 climate normals using the CLIMATE-WNA software (for details see Wang et al., 2012b).

This database was enhanced with lapse-rate based downsampling to1 km resolution to avoid over-estimating climate change effects in mountainous areas (Hamann and Wang, 2005), and increase site specificity appropriate for forecasting plant disease (Seem, 2004). Given disease observations were collected at field sites from 2003 to 2008, annual climate surfaces for this period were averaged to provide a province-wide estimate of disease risk to compare against future projections.

Climate surfaces for the 2020s, 2050s, and 2080s were generated by overlaying projections from general circulation models expressed as the difference from the 1961 to 1990 normal period. For each future period, we focused on 13 climate projections prepared for the AR4 IPCC assessment (Solomon et al., 2007) from the third Coupled Model Inter-comparison Project (Meehl et al., 2007), which incorporate the A1B, A2, and B1 SRES greenhouse gas emissions scenarios (Nakicenovic et al., 2000; Carter, 2007). The modeling groups included: BCCR-BCM2.0 (Norway), CCCMA-CGCM3.1 (Canada), CSIRO-Mk3.0 (Australia), GFDL-CM2.1 (United States), GISS-eh (United States), MIROC3.2 (hires and MEDRES) (Japan), MRI-CGCM2.3.2 (Japan), MPI-ECHAM5 (Germany), NCAR-CCSM3 (United States), UKMO-HadCM3 (United Kingdom), and UKMO-HadGEM1 (United Kingdom). All modeling groups and SRES scenarios combinations are listed in Fig. 2. These 13 models are recommended for use in British Columbia, and encompass a wide span of potential climate shifts with mean annual temperature increases ranging between 1 °C and 4 °C, and mean annual precipitation changes ranging between −5% and +15% by the 2050s, compared to the 1961–1990 period (Murdock and Spittlehouse, 2011).

2.3. Climate variable selection

Variable selection was carried out with an all-subsets regression implemented with the regsubsets( ) function within leaps package (Lumley and Miller, 2009) for the R programming environment (R Development Core Team, 2008). This method employs a branch-and-bound algorithm to perform an exhaustive search for the best subsets of input variables for predicting the response variable in multiple linear regression (Goodenough et al., 2012). Here the best linear unbiased estimate (BLUE) of disease intensity for each susceptible population at seven and 10 year site measurements was used as the response variable, and the geographic and climate variables represented the independent variables. The leaps algorithm is parameterized to output the best model at each level, where a level is defined as the number of variables considered in the model at any one time. This step prevents the results from relying on a penalty model to determine model size. The best model at each level is determined by comparing the R^2 values of the candidate models, and selecting the model with the highest R^2. Among the best models at each level, we compared the adjusted coefficients of determination (R^2_{adj}) and the root mean square error (RMSE) values to decide which set of climate variables best accounted for the variation in the field site dataset.

2.4. Model development and validation

Principle component analysis (PCA) was performed on the selected climate variables to maintain full environmental space, but remove collinearity. Variable selection with the leaps algorithm was then repeated to determine a final principal component regression model. In this final model, the best linear unbiased estimate of disease intensity of each susceptible population at each test site and measurement year represented the response variable, and the PCA components represented the independent variables. At each stage of variable selection, the Shapiro–Wilk test was used to determine if the model residuals were normally distributed ($P = 0.05$). Residuals from the principal component regression were also plotted against both the independent variables and predicted values to determine model bias.

The principle component analysis and regression were carried out with the functions princomp( ) with option cor = T and glm( ) respectively for the R programming environment (R Development Core Team, 2008). Principal component axis scores were used to generate province-wide risk maps under the aggregated 2003–2008 climate and each of the future climate projections.

The relative importance of each PCA component predictor in the overall model performance was determined by the lmg method (Lindeman et al., 1980) where R^2 is decomposed into non-negative contributions that automatically sum to the total R^2. Lmg partitions R^2 on orders of regressors using a simple unweighted average, which is considered to be an advantage over other methods (Gromping, 2007). Relative importance lmg statistic was calculated with the relaimpo package (Gromping, 2006) for the R programming environment (R Development Core Team, 2008).

The widely accepted 10-fold application (Harrell, 2001) of the K-fold cross-validation analysis was performed on the final model with the cvFit function within the cvTools package (Alfons, 2012) for the R programming environment (R Development Core Team, 2008). Here the seven and 10 year field site dataset was partitioned into 10 equal sized, stratified subsamples, where each single subsample was used as validation dataset for testing the model trained with the remaining nine subsamples. This process was repeated so that each subsample was used exactly once as the validation dataset. The aim of cross-validation is to estimate the expected level of fit of a model to a data set that is independent of the data that were used to train the model. Goodness-of-fit for the final model was calibrated with the mean square error (MSE_{cv}) averaged over the 10-folds. Further, the 10-fold cross validation was repeated 100 times to produce a more robust estimate as well as confidence intervals for the mean square error. The resulting mean square error over the repreated 10-fold cross validation indicates the measure of under- or overestimation of cedar leaf blight intensity from the final model on the observed dataset.

2.5. Western redcedar habitat and regional classes

Projected province-wide cedar leaf blight under current and future climate was reduced to areas of western redcedar habitat using the species-suitable habitat projections previously generated by Gray and Hamann (2013). For the current period, the 2003–2008 cedar leaf blight projection was overlaid with the 1961–1990 climate normals western redcedar map which closely represents the current species distribution for the province. For future climate scenarios, Gray and Hamann (2013) illustrate increased disagreement on species habitat suitability toward the 2080s, by comparing suitable habitat projections for western redcedar across 18 different climate scenarios from the AR3

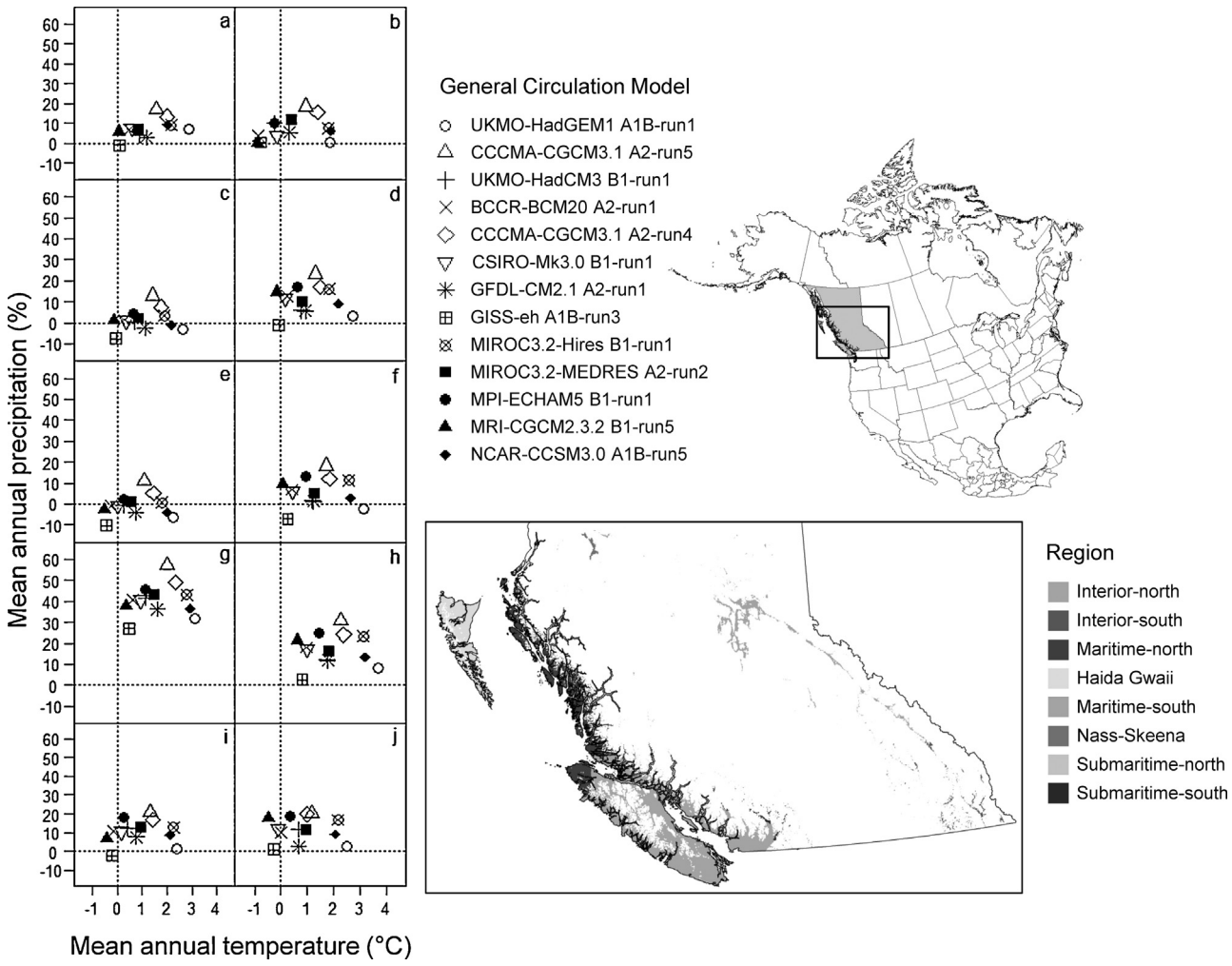

Fig. 2. Variation in projected mean annual temperature and precipitation shifts for the 2050s from current climate (2003–2008 average) among 13 climate scenarios for 10 regions of western redcedar habitat: (a) Haida Gwaii; (b) Nass-Skeena; (c) Maritime-north; (d) Maritime-south; (e) Submaritime-north-low; (f) Submaritime-south-low; (g) Submaritime-north-high; (h) Submaritime-south-high; (i) Interior-north; (j) Interior-south. Northern regions are represented in the left column of plots and each has been paired with the corresponding southern region in the right column or the low elevation equivalent. (Submaritime elevation divisions are not depicted since they are graphically small and difficult to view).

IPCC assessment (IPCC, 2007). Therefore to bound our disease projections with resonable confidence, we only considered areas where at least 70% of the models used in Gray and Hamann's study agreed habitat would be suitable for western redcedar in each future period. Although our study employed different future climate models (AR3 scenarios vs. AR4 scenarios), the differences between actual climate values from each set of models for British Columbia is minimal (Murdock and Spittlehouse, 2011). For details on the methodology and further results of the western redcedar suitable habitat model refer to Gray and Hamann (2013).

To compare model results among areas with characteristically high and low disease intensity, we divided current and projected suitable western redcedar habitat into 10 geographic regions (Fig. 2). All coastal north-south divisions were made at 51.05° latitude. Martime and Submaritime regions followed the current British Columbia western redcedar seed planning zones (Woods, 2011), with the Georgia Lowlands and Maritime seed planning zones combined. For the Maritime regions, Haida Gwaii was considered one region, and Vancouver Island north of 51.15° latitude and east of 127.58° longitude was considered north, resulting in three Maritime regions: Haida Gwaii, Maritime-north, and Maritime south. Submaritime regions were further divided by an elevation band set at 600 m, resulting in four Submaritime regions: Submaritime-north-high, Submaritime-north-low, Submaritime-south-high, and Submaritime-south-low. The elevation threshold was chosen to reflect that cedar leaf blight is rarely observed above 600 meters in these environments (J. Russell, unpubl. data). The interior western redcedar habitat was similarly divided into two regions at 51.05° latitude: Interior-north, and Interior-south. Finally, we included the Nass-Skeena, which occurs northeast of the Submaritime region, but is geographically too far west to be considered climatically similar to the Interior-north region. Size, climatic details, and a map of these regions are provided in Table 2 and Fig. 2.

3. Results

3.1. Climate trends associated with cedar leaf blight

Comparisons between field sites with cedar leaf bight present (score > 1) and absent (score = 1) show trends of warmer and wetter sites favoring increased disease (Table 1). On average, sites where the disease occurs are approximately 3 °C warmer in the winter, 1 °C warmer annually and receive 1000 mm more annual precipitation than sites where the disease is absent. Similar trends are found in the Maritime-north (M-N) and Haida Gwaii (HG) regions,

Table 2
Mean size, climate, and cedar leaf blight intensity (±standard deviation) across defined regions of western redcedar habitat in British Columbia. The values in this table reflect climate averaged over the 2003–2008 period when disease observations were collected.

	Variable	Regions[a]									
		Int-N	Int-S	M-N	HG	M-S	Nass	SM-N-h	SM-N-l	SM-S-h	SM-S-l
Location	Size (sq. km)	8623	4227	19,365	9351	40,334	831	141	565	1186	745
	Elevation (m)	770 ± 152	1152 ± 270	180 ± 172	178 ± 156	327 ± 270	403 ± 173	828 ± 210	172 ± 173	1064 ± 304	244 ± 192
Climate-general	Mean annual temperature (°C)	3.9 ± 0.7	4.3 ± 1.0	8.0 ± 0.8	7.5 ± 0.7	8.7 ± 1.1	4.4 ± 0.8	4.1 ± 1.1	7.2 ± 1.0	5.1 ± 1.2	8.3 ± 1.0
	Min winter temperature (°C)[b]	−11.1 ± 0.8	−10.6 ± 1.2	0.8 ± 1.3	0.7 ± 1.2	0.1 ± 1.4	−9.1 ± 1.0	−9.1 ± 2.4	−2.7 ± 2.3	−7.4 ± 1.7	−2.6 ± 1.8
	Mean annual precipitation (mm)	741 ± 138	830 ± 224	3675 ± 921	2628 ± 1044	2621 ± 1065	741 ± 217	1318 ± 699	2218 ± 638	1983 ± 335	1961 ± 280
Climate-in analysis	Mean summer temperature (°C)	14.3 ± 0.8	15.1 ± 1.1	13.6 ± 0.7	12.8 ± 0.6	15.5 ± 1.1	14.1 ± 0.7	13.1 ± 0.8	14.7 ± 0.8	14.7 ± 1.1	16.6 ± 1.0
	Max July temperature (°C)	22.7 ± 1.4	25.1 ± 1.5	17.5 ± 1.0	16.2 ± 0.6	21.5 ± 1.6	21.0 ± 1.0	20.7 ± 1.0	20.5 ± 1.4	22.9 ± 1.2	24.0 ± 1.4
	Max August temperature (°C)	21.6 ± 1.2	23.0 ± 1.5	18.3 ± 0.9	17.8 ± 0.6	21.4 ± 1.4	20.9 ± 1.1	20.9 ± 1.0	20.8 ± 1.3	22.0 ± 1.1	23.2 ± 1.1
	Summer climate moisture index (cm)	−9.9 ± 4.1	−14.2 ± 4.2	33.1 ± 12.8	15.7 ± 9.2	2.0 ± 11.1	−5.3 ± 2.4	−10.0 ± 11.1	4.8 ± 10.9	−9.0 ± 4.2	−8.1 ± 3.8
	Spring precipitation (mm)[c]	131 ± 26	173 ± 43	849 ± 215	606 ± 264	583 ± 260	115 ± 44	245 ± 143	450 ± 150	3909 ± 77	409 ± 68
	Summer precipitation (mm)	184 ± 28	176 ± 36	495 ± 133	309 ± 89	240 ± 96	196 ± 26	156 ± 94	268 ± 90	186 ± 32	179 ± 28
	May precipitation (mm)	49 ± 8	64 ± 14	182 ± 49	122 ± 49	105 ± 42	43 ± 6	47 ± 27	92 ± 36	86 ± 20	85 ± 18
	July precipitation (mm)	53 ± 12	33 ± 8	165 ± 44	109 ± 32	69 ± 33	70 ± 11	58 ± 30	87 ± 24	49 ± 10	49 ± 11
Disease intensity	Cedar leaf blight score (BLUE)[d]	1.5 ± 0.2	1.1 ± 0.1	4.6 ± 0.5	3.7 ± 0.4	2.5 ± 0.3	1.8 ± 0.4	1.4 ± 0.0	2.3 ± 0.2	1.4 ± 0.2	1.3 ± 0.1

[a] Region codes are as follows: Interior-north (Int-N); Interior-south (Int-S); Maritime-north (M-N); Haida Gwaii (HG); Maritime-south (M-S); Nass-Skeena (Nass); Submaritime-north-high (SM-N-h); Submaritime-north-low (SM-N-l); Submaritime-south-high (SM-S-h); Submaritime-south-low (SM-S-l).
[b] Winter temperatures were averaged over December, and January and February of the following year.
[c] Spring (March, April, May), summer (June, July, August), May and July precipitation variables are cumulative values.
[d] BLUE: best linear unbiased estimate.

which characteristically have high disease occurrence, compared to regions where cedar leaf blight is rare, such as Interior-south (Int-S) (Table 2).

3.2. Projected climate shifts for western redcedar regions

The range of projected changes in mean annual temperature and precipitation for each of the 10 regions across the 13 projected climate models for the 2050s are illustrated in Fig. 2. In this figure, northern regions are represented in the left column of plots and each has been paired with the corresponding southern region in the right column or the low elevation equivalent. Among all regions the CCCMA_CGCM3.1_A2-run5 and UKMO-HadGEM1_A1B-run1 models project the greatest increases in mean annual precipitation and temperature, respectively (Fig. 2). The ranges of projected climate shifts are fairly consistent among all regions with the exception of the Submaritime-high regions (Fig. 2g and h). For the Submaritime-north-high region, projected precipitation increase is greater than any other region, ranging between +32 and +57% (Fig. 2g). Based on model scenarios, this region could experience annual precipitation between approximately 1740 and 2070 mm by the 2050s, which is well within a standard deviation of the current mean annual precipitation of Haida Gwaii and Martime-north regions where cedar leaf blight is currently prevalent (Table 2). The Submaritime-high regions are the only two areas where mean annual temperature is projected to increase under all general circulation models (Fig. 2e and g).

3.3. Climatic variable selection and disease risk projections under current climate

The inital variable selection revealed eight climate variables that best describe the relationship between cedar leaf blight intensity and field site environments ($R^2_{adj} = 0.78$; Table 1, climate in analysis), including the most highly correlated variable, summer climate moisture index (cmiJJA, $r^2 = 0.75$). The second variable selection of PCA components reduced the number of explanatory variables to five described by:

$$\mathrm{CLB_{BLUE}} = 2.13 + 0.35 \times \mathrm{PC1} - 0.81 \times \mathrm{PC4} - 0.93 \times \mathrm{PC6} + 0.56 \times \mathrm{PC7} - 8.31 \times \mathrm{PC8} \quad (1)$$

with predicted values constrained to ≥1. The amount of variation in the observed disease intensity accounted for in the initial model was maintained in the principal component regression ($R^2_{adj} = 0.78$). Additionally, the final model had a RSME of 0.5 and all variable coefficients were found to be significant ($P < 0.001$). Model residuals were found to be normally distributed (Shapiro–Wilk = 0.15) and exhibited little apparent bias with either predicted or independent values (data not shown). The repeated 10-fold cross validation analysis produced a $\mathrm{MSE_{cv}} = 0.526$ with a confidence interval $\mathrm{CI_{MSE}} = (0.517, 0.534)$, indicating on average our model under- or overestimates cedar leaf blight intensity by half a measured score level.

Relative importance (lmg) values indicate model accuracy is overwhelmingly driven by PC1, which is approximately equally weighted among the climate variables chosen in the initial variable selection (Table 3). PC4 and PC8, which are the second and third drivers, are weighted toward temperature and climate moisture index variables, respectively (Table 3). The remaining two principle components (PC6 and PC7) reflect significant weighting toward either precipitation or temperature values (Table 3).

Projected disease intensity under 2003–2008 average climate is shown in Fig. 1. Cedar leaf blight intensity scores indicate degree of climatic suitability for a disease outbreak, where green and red indicate low- and high-risk environments, respectively. Higher

Table 3
Analysis loadings and variable importance of the components (PC) selected for the final principle component regression model for the cedar leaf blight study.

Climate variables in analysis	PC1	PC4	PC6	PC7	PC8
Average summer temperature (°C)	−0.25	−0.76	−0.03	0.08	−0.20
Maximum July temperature (°C)	−0.35	0.45	−0.12	0.66	0.21
Maximum August temperature (°C)	−0.33	0.31	−0.02	−0.74	0.19
Summer climate moisture index (cm)	0.43	−0.22	−0.33	−0.02	0.72
Cumulative spring precipitation (mm)	0.30	0.04	−0.42	0.06	−0.05
Cumulative summer precipitation (mm)	0.40	0.25	−0.33	−0.06	−0.60
Cumulative May precipitation (mm)	0.33	0.07	0.72	0.09	0.05
Cumulative July precipitation (mm)	0.39	0.06	0.26	−0.01	0.04
lmg[a]	0.67	0.17	0.03	0.01	0.11

[a] Variable importance in multiple-linear regression measured by averaging over orderings as proposed by Lindeman et al. (1980).

projected intensity along the west coast of Haida Gwaii, along the central mainland coast, and on the northern tip of Vancouver Island reflect observed responses from field trials with susceptible populations in these environments.

3.4. Projected disease risk under future climate change

Agreement among the climate projections for disease presence and absence is high for the majority of the climatically suitable western redcedar habitat for all periods (Fig. 3a). Uncertainty whether habitat will be suitable for cedar leaf blight increases slightly toward the 2080s, but only appears to occur in transition zones between areas of presence and absence confidence, for example central Vancouver Island (Fig. 3a). Decreases in the extent of species' habitat reflect increased uncertainty in western redcedar habitat projections toward the 2080s (Gray and Hamann, 2013), not absences in cedar leaf blight projections. All models agree that climate will be suitable for disease occurrence in coastal ecosystems along the mainland, Haida Gwaii and western Vancouver Island, however the disease intensity or risk of outbreak appears to decrease toward the end of the century (Fig. 3). Disease intensity is a good indication of the risk of cedar leaf blight infection. Projected disease risk was consistently highest under the MIROC3.2_MEDRES_A2-run2 climate model for the majority of suitable western redcedar habitat in each future period. Under this "worst-case-scenario", cedar leaf blight is projected to continue to cause damage in coastal areas into the 2020s (Fig. 3c) as well as appearing in northern, low elevation interior cedar-hemlock ecosystems where it is currently projected as absent (Fig. 1). This result is repeated for coastal ecosystems in the 2050s, but intensity of cedar leaf blight drastically decreases in all areas by the 2080s (Fig. 3c).

Fig. 4 illustrates the range of projected disease intensity from the 13 future climate scenarios for all regions of western redcedar habitat in the 2020s, 2050s and 2080s compared to 2003–2008 averaged climate (▲) (again projected intensity values constrained to ≥1). This image (Fig. 4) better illustrates the increase risk projected for the Submaritime-north-high and both the Submaritime-south-high and low regions, compared to Fig. 2. The current disease intensity in environments above 600 meters elevation is roughly equivalent to the 25th percentile of future projections by the 2050s (Fig. 4). A similar trend was found in both the interior regions by the 2020s and the Nass-Skeena region by the 2080s. However, while projections suggest increased disease intensity in these regions, the increase is small and will likely only be relevant if the outlying climate scenario occurs. The outlier projection for most regions is generated by the MIROC3.2_MEDRES_A2-run2 climate model (Fig. 3c), but for both Submaritime-north regions, disease projections are most severe under the UKMO-HadGEM1_A1B-run1climate model. More importantly, current disease intensity in the highly disease-affected environments, Maritime-north and Haida Gwaii, is equivalent to the 75th percentile of the range of projected values by the 2020s and the outliers by the 2080s (Fig. 4). Overall these results suggest the majority of coastal western redcedar habitat will be climatically suitable for cedar leaf blight in the future (Fig. 3a), however, if we consider the complete range of climate scenarios we used, disease intensity may potentially be low to moderate in most areas particularly over the next 70 years (Figs. 3 and 4).

4. Discussion

4.1. Variable selection illustrates how climate is strongly related to cedar leaf blight occurrence

The legitimacy of forest disease models depends on whether the variables added to the model are biologically meaningful. In this study, the branch-and-bound algorithm successfully selected climate variables that are biologically relevant for cedar leaf blight disease cycle (Table 1). Cumulative precipitation in the spring and summer as well as mean summer temperatures were shown to be important contributors to the overall model (Table 2) and are directly related to ascospore discharge and germination. Ascospores are produced from July to October, peaking between late August and early November (Sinclair et al., 1987). Sufficient moisture is required to wet apothecia initiating the discharge of matured ascospores into the environment during the production months (Kope, 2000). Germination by ascospores that have overwintered on green foliage from the previous year commonly starts when temperatures begin to rise in the spring and continues through the fall (Frankel, 1990). The branch-and-bound algorithm also selected the climate-moisture index for June through August, representing a proxy for summer humidity, for model parameterization. This is significant because the most important stage related to a disease outbreak is fungal growth, which requires a warm and moist environment to occur (Kope, 2004).

An important caveat is that our model does not consider cold temperature limits of the cedar leaf blight. Potential precipitation limitations during critical stages of the fungal life cycle and growing season limitations on reproduction could explain the rarity of disease observations in the interior and high elevation Submaritime regions; however these regions characteristically have colder winter temperatures which we suspect is a limiting factor. The pathogen has the ability to over-winter below −5 °C and continue its growth cycle the following year (Kope, 2004), but little is known about the pathogen's minimum temperature threshold. Given that warming trends are expected to be greatest in the winter months (Mbogga et al., 2009), cold thresholds that currently control disease outbreaks may no longer be effective in the future. Further research to identify the minimum cold threshold of cedar leaf blight could inform our future projections, and should be addressed to make conservative management strategies.

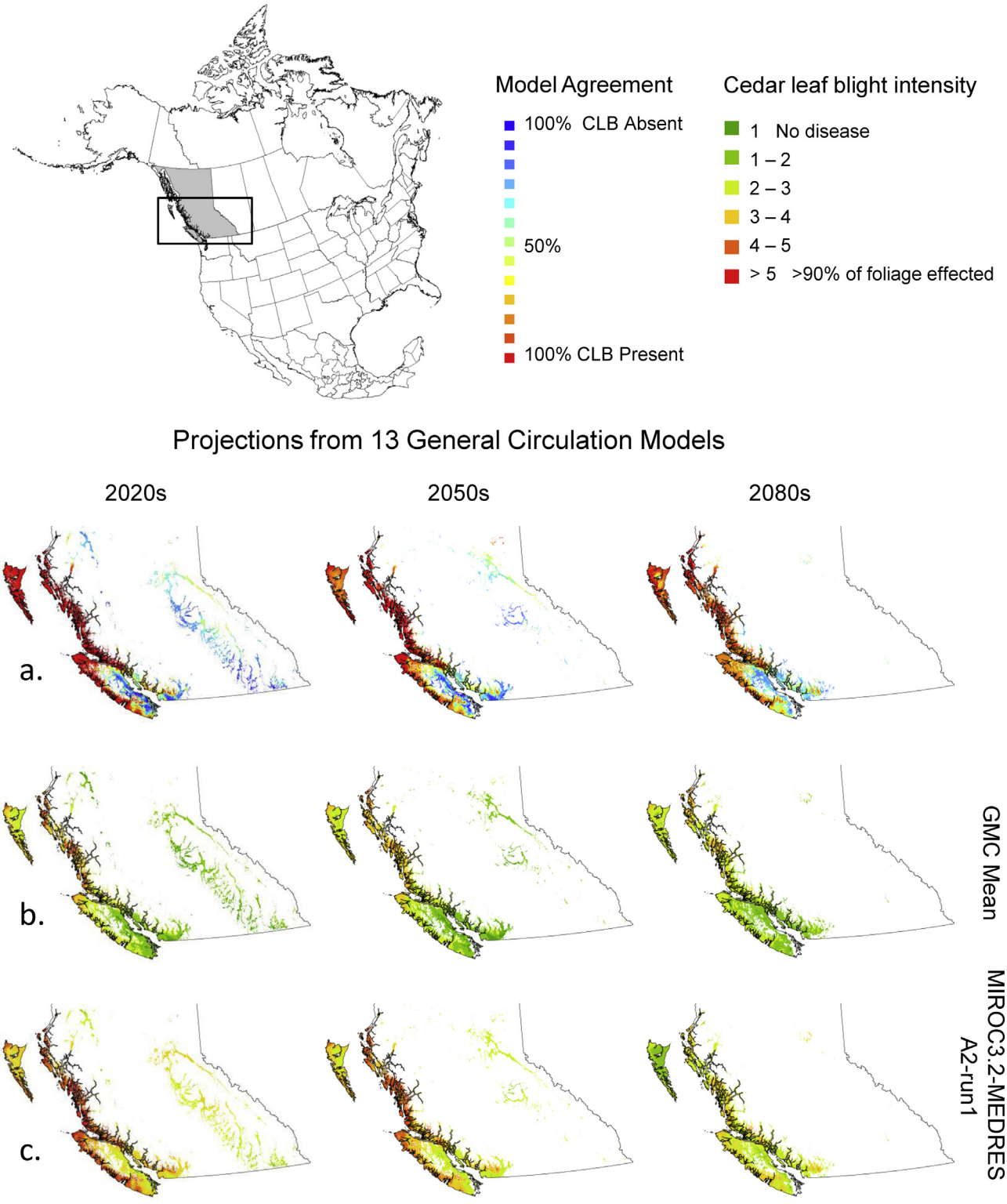

Fig. 3. Projections of cedar leaf blight (CLB) suitability under climate scenarios for the 2020s, 2050s and 2080s. (a) The degree of consensus among projections based on multiple climate change scenarios, (b) average expected disease intensity based on multiple climate change scenarios, and (c) maximum projected disease intensity under a single model which represents the "worst-case scenario". See text for a description of GMC model MIROC3.2-MEDRES A2-run2.

4.2. Future decline of disease risk could reflect climate thresholds of cedar leaf blight

Primary concerns surrounding endemic pathogens and climate change stem from the theory that "warmer and wet is better" for these infectious agents. The majority of climate scenarios we considered project both increased temperatures and precipitation for future western redcedar habitat in the province (Fig. 2). However, in most areas projected disease risk unexpectedly decreases significantly toward the 2080s (Fig. 3), compared to current

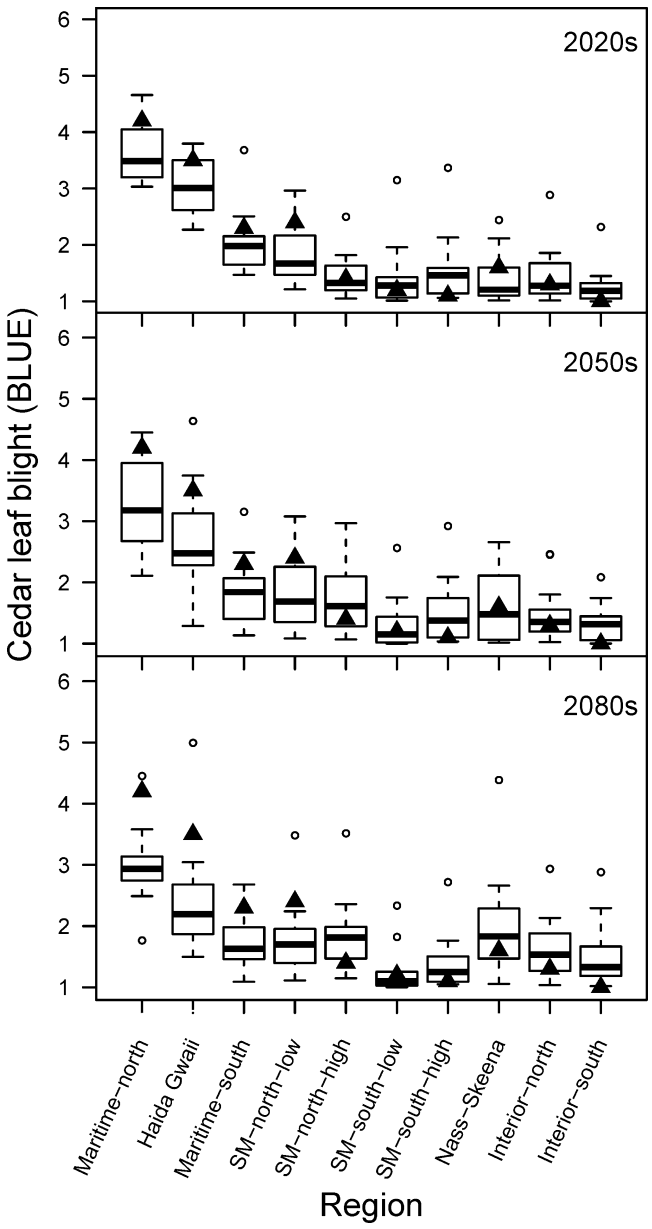

Fig. 4. Range of projected cedar leaf blight disease intensity for 10 regions of western redcedar habitat in British Columbia for the 2020s, 2050s and 2080s. For each region and period, disease intensity under the 2003–2008 averaged climates is represented as a solid triangle (▲), the projection median is represented by a solid line, and the lower and upper box edges represent the 25th and 75th percentiles for each region, respectively. Lower and upper whiskers represent the minimum and maximum projected intensity values constrained to ≥1, and upper outlier projections are indicated by an open circle (○).

projected levels (Fig. 1). Three reasons could account for this finding. First, our model could be underestimating disease risk due to poor model fit. Both the repeated 10-fold cross-validation mean square error $MSE_{cv} = 0.526$ and the adjusted coefficient of determination $R_{adj} = 0.78$ suggest the inclusion of additional variables may improve the model performance. However these values do suggest a good approximation of disease observations and out-perform multivariate regression models explaining climate-disease interactions previously reported (Watt et al., 2010).

Second, we have not considered field sites outside British Columbia, and we could therefore be excluding crucial cedar leaf blight occurrences in warmer, wetter environments in coastal Washington, Oregon, and California that may be similar to future projections. While cedar leaf blight is present in these environments (Kope, 2000) it has been rarely documented and it is considered a minor problem (USDA, 1983). We can therefore presume that the inclusion of environments external to British Columbia may adjust the presence-absence disease projections (Fig. 3a), but would have little effect on the disease intensity results (Fig. 3b and c).

Finally, the decline of disease risk under future climate change could reflect incongruities between projected climate shifts and the optimal climate thresholds for the pathogen. Kope (2004) found the temperature range for cedar leaf blight ascospore discharge and germination to be between 5 and 28 °C, with 15 °C representing the optimum. In addition, the temperature range for fungal growth within infected western redcedar was found to be between 13 and 25 °C, with 20 °C initiating accelerated growth (Pawsey, 1960). Interestingly, projected temperature increases for the 2050s support amplified ascospore discharge and germination, averaging approximately 7.5 °C in the spring, 15 °C in the summer, and 10 °C in the fall in the current high risk Maritime-north and Haida Gwaii regions (Fig. 5). Moreover, projected maximum summer temperatures range between 18 and 20 °C in current high disease risk regions for the 2050s further supporting accelerated fungal growth. However, on average, summer climate-moisture indices for all regions in the 2050s decrease by 49% with some values shifting from positive to negative (Fig. 6) indicating potential evapotranspiration will increase in all regions and, in some areas, exceed cumulative precipitation. A similar trend of reduced moisture availability can be inferred for the spring and fall seasons as summer climate moisture values are highly correlated with the values for spring and fall (spring $r^2 = 0.84$, fall $r^2 = 0.76$).

The Submaritime regions above 600 m are the only regions where projected climate moisture indices are greater than current values (Fig. 6). Correspondingly, we see the most pronounced increases in disease intensity in these regions with current measurement falling less than or equal to the 25th percentile of future projections (Fig. 4). Reduced leaf wetness can slow germination and fungal growth and eventually cause the fungus to die if persistent (Kope, 2004). Potential evapotranspiration is derived from elevation, a monthly cold temperature reduction factor, and monthly vapor pressure deficit, and is highly correlated to the maximum temperature for the period of measurement (Hogg, 1997). Projected climate shifts suggest that precipitation increases may not keep pace with expected temperature increases resulting in higher potential evapotranspiration and greater water-stress for the pathogen possibly leading to decreased disease intensity in the future.

4.3. *Range of model results should guide population selection for western redcedar reforestation*

To aid seed transfer strategies for reforestation in British Columbia, emphasis has been placed on projecting where climatically suitable habitat for the province's commercially important tree species is expected to occur under future climate change (Hamann and Wang, 2006; Gray and Hamann, 2013; Wang et al., 2012a). Projecting disease risk from climate change may refine management strategies for commercial tree species that are anticipated to maintain or expand their climatically suitable habitat; one of the most significant being western redcedar (Gray and Hamann, 2013).

Even though our model projections suggest the risk of significant damage from cedar leaf blight in western redcedar habitat will decrease in the future, adopting overly optimistic reforestation strategies may not be prudent for a number of reasons. First, while disease intensity varies among the wide range of climate scenarios, model agreement on the future climatic suitability for

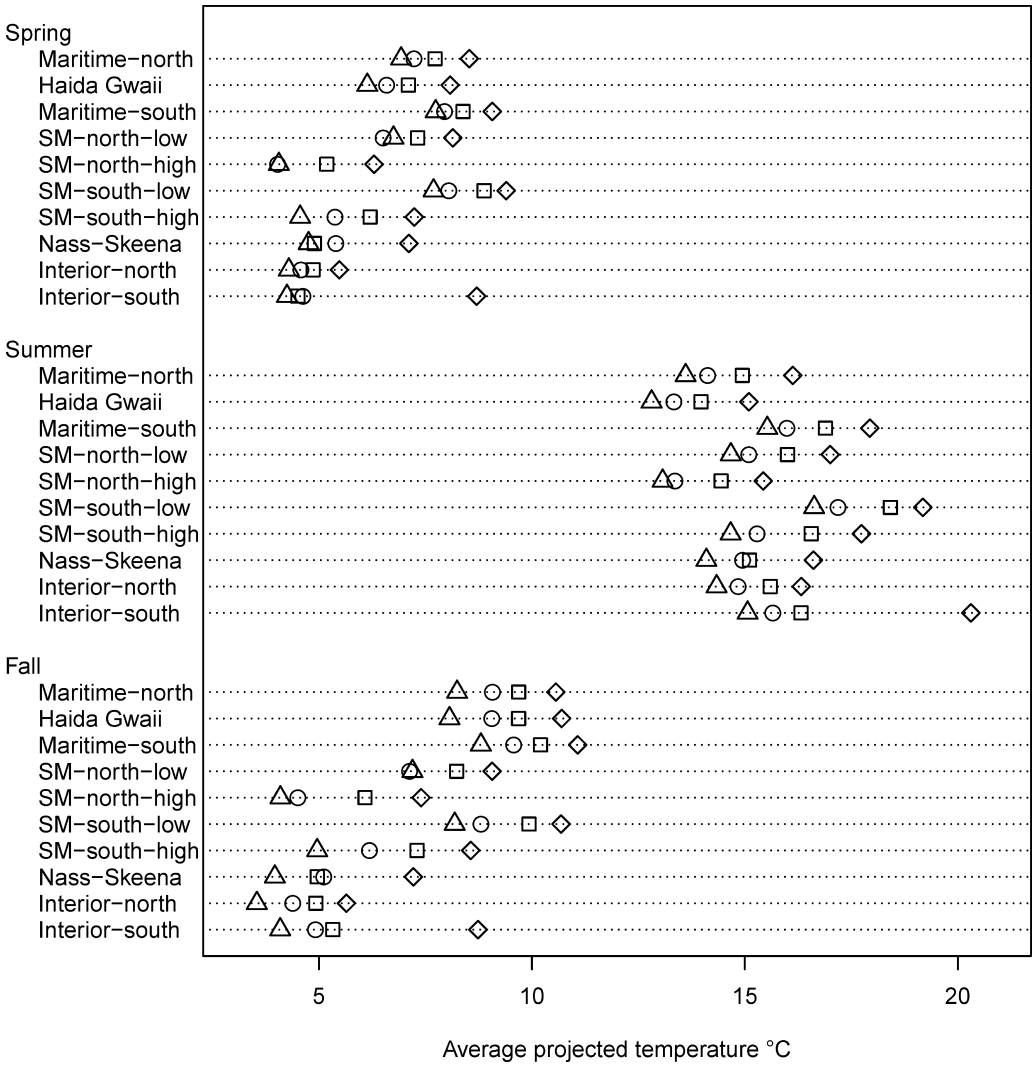

Fig. 5. Projected average spring, summer and fall temperatures for 10 regions of western redcedar habitat under 2003–2008 averaged climate (△), and a wide range of climate scenarios for the 2020s (◯), 2050s (□) and 2080s(◊).

cedar leaf blight is high for the majority of western redcedar habitat across the province (Fig. 3a). We have strong confidence that coastal ecosystems will be suitable for the disease to occur, and if the "worst-case scenario" transpires (Fig. 3c), there is considerable risk that cedar leaf blight will cause significant damage to trees in these ecosystems as well as in interior regions where cedar leaf blight currently does not occur (Fig. 4). Climate under our "worst-case scenario", MIROC3.2_Hires_B1-run2, signifies a moderate 1–1.5 °C mean annual temperature rise and a 2–10% mean annual precipitation increase by the 2050s (Fig. 2). Comparable

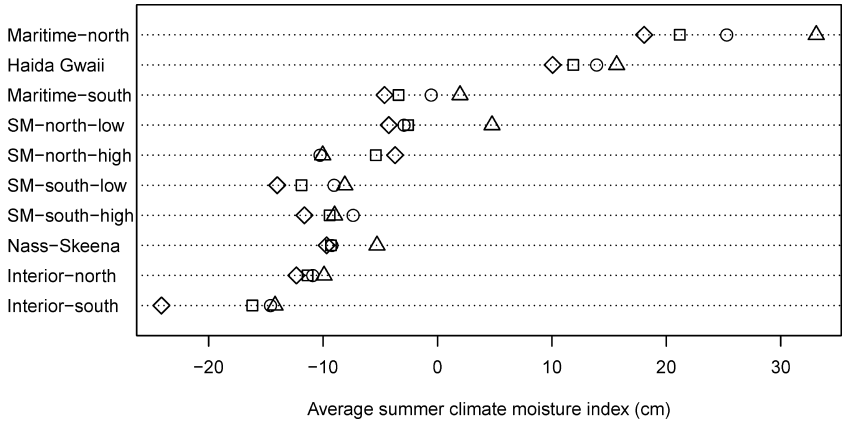

Fig. 6. Projected summer climate moisture index for 10 regions of western redcedar habitat under 2003–2008 averaged climate (△), and a wide range of climate scenarios for the 2020s (◯), 2050s (□) and 2080s(◊).

increases of approximately 2 °C mean annual temperature and 12% mean annual precipitation have been observed in British Columbia from approximately 1975–2000 (Mbogga et al., 2009), suggesting that "worst-case" climate shifts could very likely materialize. Moreover, if temperature slightly exceeds past shifts and follows the 2–3.5 °C mean annual temperature rise projected by the UKMO-HadGEM1_A1B-run1 climate model, the northern Submaritime regions may also experience higher disease intensity (Fig. 4).

Second, due to the long-lived nature of forest trees, little is known about the selective and evolutionary forces that determine the balance between the predictability of infection and selective intensity in forest ecosystems (Burdon et al., 2012). Climate change will affect how temperature and precipitation favor the pathogen, the tree species, or both. For example, forest pathogens may overwhelm ecosystems as their ability to adapt to new climates is far greater than their long-lived hosts (Sturrock et al., 2011). In contrast, elevated CO_2 may increase host resistance to disease as was observed with loblolly pine (*Pinus taeda*) and northern red oak seedlings (*Quercus rubra*) to fusiform rust fungus (*Cronartium quercuum* f. sp. *fusiforme*) and pitch canker fungus (*Fusarium circinatum*) in the southern United States (Runion et al., 2010). Unforeseen environmental shifts that favor cedar leaf blight could therefore result in elevated levels of disease and significant maladaptation and mortality not represented in the model projections.

Third, influxes in disease outbreaks may be driven by daily, small scale or accumulated climate events which are difficult to accurately measure and predict at a provincial level. For example, neighboring trees may experience vastly different water availability, depending on overstory cover, which could greatly affect their infection rate and the potential for ascospore germination.

Fourth, climate is not homogenous across some of the broader regions we defined in this study. Disease outbreaks in key microsites could therefore have been outweighed when considering the regional average. For example, in the Maritime-south region, the eastern coast of Vancouver Island is categorized as very dry or moist Maritime habitat, but the western coast is categorized as very wet Montane and Submontane environments. Correspondingly, cedar leaf blight occurs at very low levels or is absent on the eastern coast and higher elevations, but is prevalent at moderate to high levels on the western coast as evidence by our Maritime south region test sites. Projections suggest cedar leaf blight intensity in the Maritime-south region will range between 1 (CLB absent) and 4 (CLB moderate-high intensity) in the future, however we would expect there will be key microsites where disease intensity will be notably higher than the regional average.

Finally, cedar leaf blight is most damaging to young seedlings (Frankel, 1990; Kope, 2004). Under the worst case scenario, averaged disease intensity projections for the 2020s and 2050s show a level 3 or greater for the majority of the west coast of Haida Gwaii and the northern tip of Vancouver Island (Fig. 3c). At these intensities, cedar leaf blight can cause up to 40% reduction in growth on seven to 10 year-old trees (data not shown). This was also shown by the negative correlation between CLB breeding values and height in Russell and Yanchuk (2012).

All of the above suggests that deployment strategies for coastal low elevation areas should consider disease resistant populations. Current geographically-based seed transfer for wildstand western redcedar in the Maritime seed planning zone allows seedlots to be moved 600 m upwards and 400 m downwards in elevation, and 3° latitude north and south from point of origin (Snetsinger, 2005). These relatively relaxed transfer guidelines are a result of previous studies that have indicated minimal population variation related to seed origin in growth and physiological traits (Cherry and Lester, 1992; Rehfeldt, 1994; Grossnickle et al., 2005; Russell and Krakowski, 2010). However, population variation in cedar leaf blight resistance appears more adaptive than for general growth traits, such that trees from milder and wetter ecosystems were more resistant to the disease (Russell et al., 2007; Russell and Krakowski, 2010). This, in conjunction with our results, would suggest that current transfer guidelines may not be appropriate when considering cedar leaf blight infection. Movement of wildstand southern populations northward and of populations over 500 m elevation downward should be avoided. For reforestation in susceptible environments, the use of resistant wildstand populations may be an efficient management strategy to minimize the probability of cedar leaf blight outbreaks. However, in the southern portion of coastal British Columbia, the majority of western redcedar stock used in reforestation originates from seed orchard lots that include parents tested for volume. These seedlots can be transferred freely within the Maritime seed planning zone (SPZ) up to 700 m elevation and between 48° and 52° N latitude. Cedar leaf blight severity has an on-significant genetic correlation with growth (Russell and Yanchuk, 2012), resulting in current orchard seedlots not having any substantive improvements in cedar leaf blight resistance.

For all disease risk assessments, resilience to negative surprises should be the most important policy aim (Shaw, 2009). Therefore, results of model projections from this study can be used as a guide to making reforestation investments with cedar leaf blight-resistant stock while considering a wide range of potential climate shifts for the province. In addition, disease intensity projections under current climate could be used to identify areas that have most likely historically been under significant disease pressure where new resistant western redcedar populations could be found to enhance breeding programs. As more incident data on cedar leaf blight is accumulated, and as climate models and global circulation model predictions improve, these models can be refined over time to provide a very dynamic tool to further evaluate and adjust deployment decisions for western redcedar.

Acknowledgements

We would like to thank the NSERC CREATE Program in Forests and Climate Change for funding this research. Additionally we would like to sincerely thank Jake King for developing the field CLB rating system and recording the ratings on tens of thousands of trees across BC, Craig Ferguson and Jodie Krakowski for data management, Harry Kope for his advice and assistance with the species pathology, and Andreas Hamann for access to spatial software.

References

Alfons, A., 2012. cvTools: Cross-Validation Tools for Regression Models. R Package Version 0.3.2, URL http://CRAN.R-project.org/package=cvTools

Ayers, M.P., Lombardero, M.J., 2000. Assessing the consequences of global change for forest disturbance from herbivores and pathogens. Sci. Total Environ. 262, 263–286.

Bergot, M., Cloppet, E., Pernaud, V., Deque, M., Marcais, B., Desprez Loustau, M., 2004. Simulation of potential range expansion of oak disease caused by *Phytophthora cinnamomi* under climate change. Global Change Biol. 10, 1539–1552.

Boland, G.J., Melzer, M.S., Hopkin, A., Higgins, V., Nassuth, A., 2004. Climate change and plant diseases in Ontario. Can. J. Plant. Pathol. 26, 335–350.

Bourgeois, G., Bourque, A., Deaudelin, G., 2004. Modelling the impact of climate change on disease incidence: a bioclimatic challenge. Can. J. Plant Pathol. 26, 285–290.

Bradshaw, R.E., 2004. Dothistroma (red-band) needle blight of pines and the dothistromin toxin: a review. Forest Pathol. 34, 163–185.

Burdekin, D.A., Phillips, D.H., 2008. Chemical control of *Didymascella thujina* on western red cedar in forest nurseries. Ann. Appl. Biol. 67, 131–136.

Burdon, J.J., Thrall, P.H., Nemri, A., 2012. Approaches to understanding the impact of life-history features on plant-pathogen co-evolutionary dynamics. In: Sniezko, R., YanchukF A.D., Kliejunas, J.T., Palmieri, K.M., Alexander, J.M., Frankel, S.J. (Eds.), Proceedings of the Fourth International Workshop on the Genetics of Host–Parasite Interactions in Forestry: Disease and Insect Resistance in Forest Trees. Gen. Tech. Rep. PSW-GTR-240. Pacific Southwest Research Station, Forest Service, U.S. Department of Agriculture, Albany, CA, pp. 104–111, p. 372.

Carter, T.R., 2007. General Guidelines on the Use of Scenario Data for Climate Impact and Adaptation Assessment. Version 2. Task Group on Data and Scenario

Support for Impact and Climate Assessment, Intergovernmental Panel on Climate Change.
Cherry, M.L., Lester, D.T., 1992. Genetic variation in *Chamaecyparis nootkatensis* from coastal British Columbia. West. J. Appl. Forerst. 7, 25–29.
Daly, C., Halbleib, M., Smith, J.I., Gibson, W.P., Doggett, M.K., Taylor, G.H., Curtis, J., Pasteris, P.P., 2008. Physiographically sensitive mapping of climatological temperature and precipitation across the conterminous United States. Int. J. Climatol. 28, 2032–2064.
Desprez-Loustau, M.-L., Marcais, B., Nageleisen, L.M., Ouiym, D., Vannini, A., 2006. Interactive effects of drought and pathogens in forest trees. Ann. For. Sci. 63, 597–612.
Dukes, J.S., Pontius, J., Orwig, D., Garnas, J.R., Rodgers, V.L., Brazee, N., Cooke, B., Theoharides, K.A., Stange, E.E., Harrington, R., Ehrenfeld, J., Gurevitch, J., Lerdau, M., Stinson, K., Wick, R., Ayres, M., 2009. Responses of insect pests, pathogens, and invasive plant species to climate change in the forests of northeastern North America: what can we predict? Can. J. For. Res. 39, 231–248.
Frankel, S., 1990. Evaluation of Fungicides to Control Cedar leaf blight on western red cedar at Hombolt Nursery. Forest Pest Management Report No. 90-01. USDA Forest Service, Pacific Southwest Region, 4pp.
Gilmour, A.R., Gogel, B.J., Cullis, B.R., Welham, S.J., Thompson, R., 2009. ASReml User Guide. Release 3.0. VSN International, Hemel Hempstead.
Goodenough, A.E., Hart, A.G., Stafford, R., 2012. Regression with empirical variable selection: description of a new method and application to ecological datasets. PLoS ONE 7, e34338, doi:10.1371/journal.pone.0034338.
Gray, L.K., Hamann, A., 2013. Tracking suitable habitat for tree populations under climate change in western North America. Clim. Change 117, 289–303.
Gromping, U., 2006. relaimpo: Relative Importance of Regressors in Linear Models. R Package Version 1.1-1, URL http://CRAN.R-project.org/package=relaimpo
Gromping, U., 2007. Estimators of relative importance in linear regression based on variance decomposition. Am. Stat. 61, 139–147.
Grossnickle, S.G., Fan, S., Russell, J.H., 2005. Variation in gas exchange and water use efficiency patterns among populations of western redcedar. Trees-Struct. Funct. 19, 32–42.
Hamann, A., Wang, T., 2005. Models of climate normals for genecology and climate change studies in British Columbia. Agric. For. Meteorol. 128, 211–221.
Hamann, A., Wang, T., 2006. Potential effects of climate change on ecosystem and tree species distribution in British Columbia. Ecology 87, 2773–2786.
Harrell, F.E., 2001. Regression Modeling Strategies: With Applications to Linear Models, Logistic Regression, and Survival Analysis. Springer-Verlag, Inc., New York, NY.
Hogg, E.H., 1997. Temporal scaling of moisture and the forest-grassland boundary in western Canada. Agric. For. Meteorol. 84, 115–122.
IPCC, 2007. Climate Change 2007: The Physical Basics (Summary for Policymakers). Intergovernmental Panel on Climate Change, ISBN 9780521 70596-7.
Kelly, M., Guo, Q., Liu, D., Shaari, D., 2007. Modeling the risk for a new invasive forest disease in the United States: an evaluation of five environmental niche models. Comput. Environ. Urban 31, 689–710.
Kope, H.H., Sutherland, J.R., 1994. Keithia blight: review of the disease, and research on container-grown, western redcedar in British Columbia, Canada. In: Perrin, R., Sutherland, J.R. (Eds.), Disease and insects in forest nurseries. Proceedings of the 2nd Meeting of the IUFRo Working Party. S2.07-09. 3–10 October 1993, Dijon, France. Institute National de la Recherche Agronomique, Versailles, France, pp. 27–44.
Kope, H.H., Sutherland, J., Trotter, D., 1996. Influence of cavity size, seedling growing density and fungicide applications on Keithia blight of western redcedar seedling growth and field performance. New Forest. 11, 137–147.
Kope, H.H., 1998. Analysis of proteins of disease-free and *Didymascella thujina*-infrested leaves of western red cedar (*Thujia plicata*). Plant Dis. 82, 210–212.
Kope, H.H., Trotter, D., 1998a. Evaluation of mancozeb and propiconazole to control Keithia leaf blight of container-grown western red cedar. For. Chron. 74, 583–587.
Kope, H.H., 2000. *Didymascella thujina*. Can. J. Plant Pathol. 22, 407–409.
Kope, H.H., 2004. *Didymascella thujina*. In: Forestry Compendium, 2005 Edition. CAB International, Wallington, UK.
Lindeman, R., Merenda, P., Gold, R., 1980. Introduction to Bivariate and Multivariate Analysis. Scott Foresman, and Company, Glenview, IL.
Lines, R., 1988. Choice of seed origins for the main forest species in Britain: eastern redcedar UK. Forest. Comm. Bull. 66, 37–38.
Lumley, T., Miller, A., 2009. leaps: Regression Subset Selection. R package Version 2.7, URL http://CRAN.R-project.org/package=leaps
Madden, L.V., Hughes, G., van den Bosch, F., 2007. The Study of Plant Disease Epidemics. APS Press, St. Paul, MN.
Mbogga, M.S., Hamann, A., Wang, T., 2009. Historical and projected climate data for natural resource management in western Canada. Agric. For. Meteorol. 149, 881–890.
Meehl, G.A., Covey, C., Taylor, K.E., Delworth, T., Stouffer, R.J., Latif, M., McAvaney, B., Mitchell, J.F.B., 2007. The WCRP CMIP3 multimodel dataset: a new era in climate change research. Bull. Am. Meteorol. Soc. 88, 1383–1394.
Meentemeyer, R.K., Anacker, B.L., Mark, W., Rizzo, D.M., 2008. Early detection of emerging forest disease using dispersal estimation and ecological niche modeling. Ecol. Appl. 18, 377–390.
Moore, B., Green, J.L., 1976. Leaf-browning and shedding-Arbor-Vitae and Juniper. Ornamentals Northwest Achieve 1, 1–2.
Murdock, T.Q., Spittlehouse, D.L., 2011. Selecting and Using Climate Change Scenarios for British Columbia. Pacific Climate Impacts Consortium. University of Victoria, Victoria, BC, 39 pp.
Nakicenovic, N., Alcamo, J., Davis, G., de Vries, B., Fenhann, J., Gaffin, S., Gregory, K., Grübler, A., Jung, T.Y., Kram, T., La Rovere, E.L., Michaelis, L., Mori, S., Morita, T., Pepper, W., Pitcher, H., Price, L., Raihi, K., Roehrl, A., Rogner, H.-H., Sankovski, A., Schlesinger, M., Shukla, P., Smith, S., Swart, R., van Rooijen, S., Victor, N., Dadi, Z., 2000. IPCC Special Report on Emissions Scenarios. Cambridge University Press, Cambridge, United Kingdom and New York, NY, USA, 599 pp.
Pawsey, R.G., 1960. An investigation into Keithia disease of *Thuja plicata*. Forestry 33, 174–186.
Porter, W.A., 1957. Biological Studies on Western Redcedar Blight Caused by *Keithia thujina* Durand. Canada Department of Agriculture, Forest Biology Division, Victoria, BC, Interim report.
R Development Core Team, 2008. R: A Language and Environment for Statistical Computing. R Foundation for Statistical Computing, Vienna, Austria, ISBN 3-900051-07-0.
Rehfeldt, G., 1994. Genetic structure of western redcedar populations in the interior west. Can. J. For. Res. 24, 670–680.
Runion, G.B., Prior, S.A., Rogers, H.H., Mitchell, R.J., 2010. Effects of elevated atmospheric CO_2 on two southern forest diseases. New Forest. 39, 275–285.
Russell, J.H., Kope, H.H., Ades, P., Collinson, H., 2007. Variation in cedar leaf blight (*Didymascella thujina*) resistance of western redcedar (*Thuja plicata*). Can. J. For. Res. 37, 1978–1986.
Russell, J.H., Krakowski, J., 2010. Yellow-cedar and western redcedar adaptation to present and future climates. In: Proceedings a Tale of Two Cedars: International Symposium on Yellow-cedar and Western Redcedar PNW GTR-828.
Russell, J.H., Yanchuk, A.D., 2012. Breeding for growth improvement and pest resistance in *Thuja plicata*. In: Proceedings of the 4th International Workshop on Genetics of Host-Parasite Interactions in Forestry. Gen. Tech. Rep. PSW-GTR-240, Pacific Southwest Research Station, Forest Service. U.S. Department of Agriculture, Albany, CA.
Seem, R.C., 1984. Disease incidence and severity relationships. Annu. Rev. Phytopathol. 22, 133–150.
Sinclair, W.A., Lyon, H.H., Johnson, W.T., 1987. Diseases of Trees and Shrubs. Cornell University Press, Ithaca, NY.
Snetsinger, J., 2005. Chief Forester's Standards for Seed Use. BC Ministry of Forests, Victoria, BC.
Soegaard, B., 1956. Leaf blight resistance in Thujia. In: Yearbook 1956. Royal Veterinary and Agricultural College, Copenhagen, Denmark, pp. 30–48.
Sturrock, R.N., Frankel, S.J., Brown, A.V., Hennon, P.E., Kliejunas, J.T., Lewis, K.J., Worrall, J.J., Woods, A.J., 2011. Climate change and forest diseases. Plant. Pathol. 60, 133–149.
Seem, R.C., 2004. Forcasting plant disease in a changing climate: a question of scale. Can. J. Plant Pathol. 26, 274–283.
Shaw, M., 2009. Preparing for changes in plant disease due to climate change. Plant Prod. Sci. 45, S3–S10.
Solomon, S., Qin, D., Manning, M., Marquis, M., Averyt, K., Tignor, M.M.B., Miller Jr., H.L., Chen, Z. (Eds.), 2007. Climate Change 2007: The Physical Science Basis. Cambridge University Press, Cambridge UK, 996 pp.
Trotter, D., Shrimpton, G., Kope, H.H., 1994. The effects of Keitha blight on outplanting performance of western redcedar container seedlings at two reforestation sites in British Columbia – preliminary results. In: Landis, T.D., Dumroese, R.K. (Eds.), National Proceedings, Forest and Conservation Nursery Association. General Technical Report. RM-257. US Department of Agriculture, Forest Service, Rocky Mountain Forest and Range Experiment Station, Fort Collins, CO, pp. 196–202.
USDA, 1983. Forest Disease Management Notes. Pacific Northwest Region, USDA Forest Service, Portland, OR, 54 p.
Venette, R.C., Cohen, S.D., 2006. Potential climatic suitability for establishment of *Phytophthora ramorum* within the contiguous United States. Forest Ecol. Manag. 231, 18–26.
Venette, R.C., 2009. Implication of global climate change on the distribution and activity of *Phytophthora ramorum*. In: McManus, K.A., Gottschalk, K.W. (Eds.), Proceedings of the 20th U.S. Department of Agriculture Interagency Research Forum on Invasive Species 2009. General Technical Report NRS-P-51. US Department of Agriculture, Forest Service, Northern Research Station, Newtown Square, PA, pp. 58–59.
Watt, M.S., Stone, J.K., Hood, I.A., Palmer, D.J., 2010. Predicting the severity of Swiss needle cast on Douglas-fir under current and future climate in New Zealand. Forest Ecol. Manag. 260, 2232–2240.
Wang, T., Campbell, E.M., O'Neill, G.A., Aitken, S.N., 2012a. Projecting future distributions of ecosystem climate niches: uncertainties and management applications. Forest Ecol. Manag. 279, 128–140.
Wang, T., Hamann, A., Spittlehouse, D., Murdock, T.N., 2012b. ClimateWNA – high-resolution spatial climate data for western North America. J. Appl. Meteorol. Clim. 61, 16–29.
Woods, J., 2011. Forest Genetics Council of BC Business Plan 2011/12. SD399.5.B74. Forest Genetics Council of BC, Victoria, BC.
Woods, A., 2003. Species diversity and forest health in northwest British Columbia. For. Chron. 79, 892–897.
Woods, A., Coates, K.D., Hamann, A., 2005. Is an unprecedented dothistroma needle blight epidemic related to climate change? Bioscience 55, 761–769.